ChemPubSoc Europe

DOI: 10.1002/cctc.201300853

Aryl Sulfotransferase from *Haliangium ochraceum*: A Versatile Tool for the Sulfation of Small Molecules

Iván Ayuso-Fernández, Miquel A. Galmés, Agatha Bastida, and Eduardo García-Junceda*[a]

Sulfation is an important molecular modification that regulates essential cellular processes and is also implicated in numerous pathological processes. The enzymes responsible for this reaction in living organisms are sulfotransferases. The gene Hoch_5094 from *Haliangium ochraceum* is annotated as a putative sulfotransferase. The arylsulfotransferase codified by this gene (HocAST) was expressed heterologously in *E. coli* and showed aryl sulfotransferase activity. Circular dichroism analysis of HocAST showed a main α/β secondary structure that agrees with the overall structure of other cytosolic sulfotransferases. Interestingly, HocAST was able to use both *p*-nitrophenyl sulfate and 3′-phosphoadenosine-5′-phosphosulfate (PAPS) as sulfuryl donors contrary to that of aryl sulfate sulfotransferase, which cannot use PAPS as a donor. Regarding the specificity towards the acceptor, HocAST has shown quite a wide scope and was able to accept several mono- and dihydroxylated phenols and other phosphorylated compounds as substrates.

Introduction

Sulfation is an important molecular modification in all living organisms that regulates essential cellular processes and is also implicated in numerous pathological processes.[1] The enzymes responsible for this reaction in living organisms are sulfotransferases (EC 2.8.2.-). These enzymes catalyze the transfer of a sulfuryl moiety (SO_3^-) from 3′-phosphoadenosine-5′-phosphosulfate (PAPS) to the hydroxyl and primary amine groups of a variety of acceptors. In eukaryotes, two classes of sulfotransferases have been described: Golgi-membrane sulfotransferases (STs), which sulfate large molecules such as polysaccharides and proteins, and cytosolic sulfotransferases (SULTs), which transfer the sulfuryl group from PAPS to phenols, steroids, hormones, amines, and xenobiotics. This latter family is also known as phenol or aryl sulfotransferases (ArylST).[2] In addition to these two families, a group of PAPS-independent sulfotransferases that use two aryl substrates, one as a sulfuryl donor and the other one as an acceptor, have been described in bacteria. Although the bacterial aryl sulfate sulfotransferase (ASST) was first described in commensal intestinal bacteria as early as 1986, the identity of the natural donor has not been clearly established.[3]

From a synthetic point of view, STs are attractive because of their ability to sulfate, in a regio- and stereoselective manner, complex polysaccharides such as glycosaminoglycans (GAGs), which are polymers that play crucial roles in the development and organogenesis and thus seem to be essential for multicellular life.[4] However, the synthetic use of STs is hampered because of the high cost and instability of PAPS and the problem of product inhibition caused by 3′-phosphoadenosine-5′-phosphate (PAP).[5] In addition to their use for the sulfation of different flavonoids, steroids, peptides, and aliphatic alcohols,[6] ArylST, in particular rat liver aryl sulfotransferase IV (Ast IV), has been used to develop a one-enzyme regeneration system for PAPS (Scheme 1).[7] This cycle is based on the reversibility of the reaction catalyzed by the ArylST.[8] Thus, if coupled to another PAPS-dependent sulfotransferase, the ArylST can transfer the sulfuryl group from *p*-nitrophenyl sulfate (*p*-NPS) to PAP to regenerate PAPS in situ and overcome the inhibition by PAP. However, scale-up of this regeneration system is hampered by

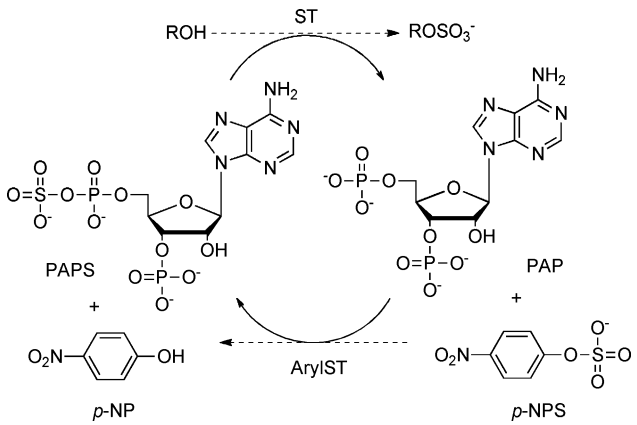

Scheme 1. PAPS regeneration cycle based on the use of aryl sulfotransferases.

[a] *I. Ayuso-Fernández,[+] M. A. Galmés, Dr. A. Bastida, Dr. E. García-Junceda*
Departamento de Química Orgánica Biológica
Instituto de Química Orgánica General, CSIC
Juan de la Cierva 3, 28006 Madrid (Spain)
Fax: (+34) 915-644-853
E-mail: eduardo.junceda@csic.es

[+] *Current address:*
Departamento de Biología Medioambiental
Centro de Investigaciones Biológicas, CSIC
Ramiro de Maeztu 9, 28040 Madrid (Spain)

Supporting information for this article is available on the WWW under http://dx.doi.org/10.1002/cctc.201300853.

the poor stability of the pure Ast IV.[6c] Therefore, the search for a new ArylST with better properties as a biocatalyst is ongoing. In this sense, the gene Hoch_5094 from the bacteria *Haliangium ochraceum* codifies for a putative aryl sulfotransferase. Herein, we describe the heterologous expression of the gene Hoch_5094 in *Escherichia coli* and the biochemical characterization of the gene product as well as a preliminary analysis of its donor and acceptor specificity.

Results and Discussion

Sequence analysis of the aryl sulfotransferase from *Haliangium ochraceum*

In recent years the number of complete genomes, especially from bacteria that have been sequenced, has grown dramatically, which provides a unique source to find new enzymes. *Haliangium ochraceum* is the type species of the genus *Haliangium* in the myxococcal family *Haliangiaceae* and its genome has been sequenced recently.[9] The product of the gene Hoch_5094 is annotated as a putative sulfotransferase because of the sequence homology with the family SULT_1 (Pfam00685).[10] As there is no experimental evidence of the activity of this enzyme, we decided to undertake a comparative analysis of its sequence with the well-characterized SULT from human (HsSULT1A1a), rat (RnSULT1A1), and mouse (MmSULT1D1). The domains that define the phenol sulfotransferase activity[11] are shown in Figure 1.

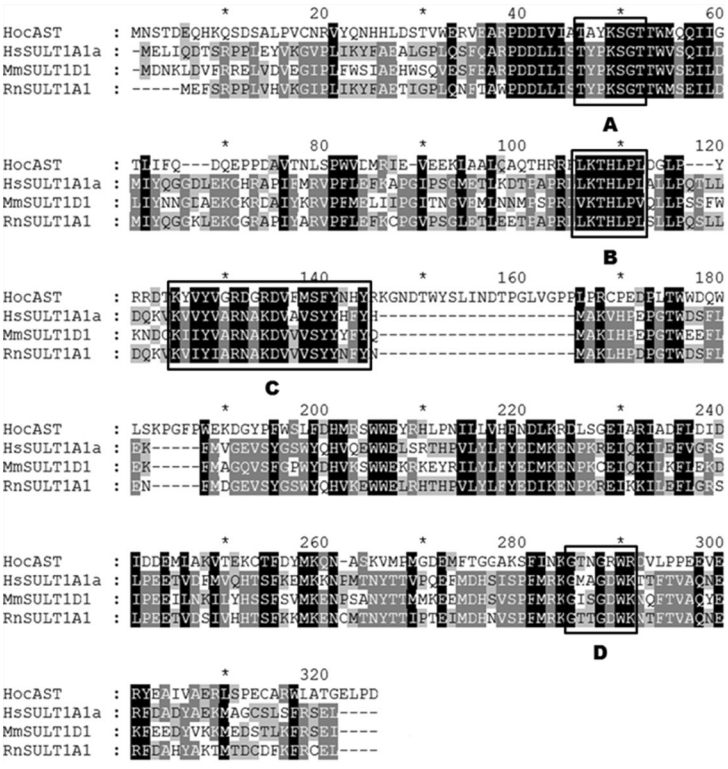

Figure 1. Alignment of the amino acid sequence of the hypothetical aryl sulfotransferase from *Haliangium ochraceum* versus three known sulfotransferases. The boxes A, B, C, and D frame the conserved regions involved in the aryl sulfotransferase activity.

A: This domain is known as the phosphosulfurile binding site (PBS) and interacts with the 5′-phosphate group from PAPS to point the sulfuryl donor to the acceptor in the active site.

B: This highly conserved region includes the catalytic histidine (H105 in HocAST). It is expected that the amino acids in this domain contribute significantly to the structure of the active center.

C: In HsSULT1 A1a R130 and S138 interact with the 3′-phosphate group of PAPS. In addition, S138 avoids the hydrolysis of PAPS in the absence of an acceptor substrate.

D: This domain contains the motif GxxGxWK, which is highly conserved in this kind of sulfotransferase. This sequence interacts with the 3′-phosphate group of PAPS and, together with domain C, stabilizes its binding to the active site. In HocAST there is an R instead of the K but as both amino acids are basic and have similar properties, it can be expected that the role of this domain is conserved in this enzyme.

We performed automated protein structure homology modeling by using the SwissModel[12] server using the protein SULT1D1 from *Mus musculus* (PDB entry 2zyt) as a template.[13] The folding of HocAST is highly conserved if superposed to other sulfotransferases, the structures of which have been solved already. The topology of HocAST folding was β1, α1, α2, α3, β2, β3, α4, β4, β5, α5, α6, β6, α7, α8, α9, α10, α11, α12, which is virtually identical to the topology of the SULT proteins (Figure 2 A). To confirm that the catalytic residue of the HocAST could be His105 (deduced by alignment), we performed docking studies of the model protein with PAP and *p*-NPS and obtained a glide score of -8.59 kcal mol^{-1} (Figure 2 B).[14] In the HocAST–PAP complex, the 5′-phosphate group of PAP is positioned in an analogous manner to the phosphate group of PAPS in the crystallographic MmSULT1D1–PAPS complex (Figure S1). In both cases, the phosphate groups are 3 Å from the catalytic His residue (His105in HocAST and His108in MmSULT1D1).

Therefore, as HocAST presented the main structural characteristics and an overall 3D structure in agreement with the cytosolic sulfotransferases, we decided to perform its expression in *E. coli* to perform a detailed structural and functional analysis as well as to explore its synthetic applicability.

Expression and structural characterization of HocAST

The gene Hoch_5094 was amplified by polymerase chain reaction (PCR) from the genomic DNA of *Haliangium ochraceum* using primers designed to complement specifically 25 base pairs (bp) at the 5′ end of the codifying and complementary DNA strains. The recognition sequence for the restriction enzymes *Nde*I and *Xho*I were introduced into the amplification product during PCR. The resulting amplified band had the expected size (954 bp) and was digested and introduced into the expression vector pET-28b(+),

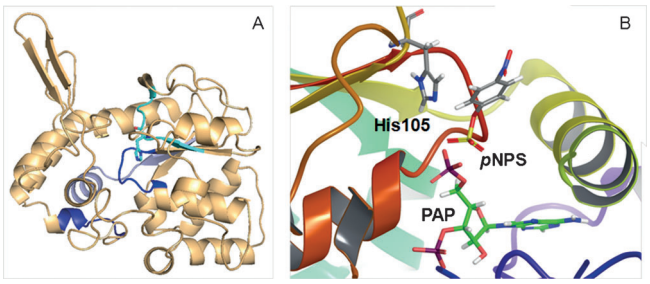

Figure 2. A) Modeling the tertiary structure of the protein HocAST; the reactive His105 is shown in sticks and the conserved motifs in color: Box A, density blue; Box B, cyan; Box C, deep blue, and Box D, light blue; B) Docking of *p*-NPS and PAP in the HocAST model.

which introduces a six-histidine tag at the N terminus of the recombinant protein.

E. coli BL21 (DE3) cells were transformed with this plasmid, and the expression of recombinant protein was induced with 0.5 mM isopropyl β-D-1-thiogalactopyranoside (IPTG) at an optical density at 600 nm (OD_{600nm}) of 0.5–0.6. Sodium dodecyl sulfate polyacrylamide gel electrophoresis (SDS-PAGE) of HocAST expression showed a band of the expected molecular mass (37 kDa) in the soluble fraction that represented 70% of the total protein. HocAST was purified by immobilized metal-affinity chromatography (IMAC) through the His-tag.

The purified recombinant protein presented a mass of 37 221 Da, and the peptide mass fingerprint showed 18 peptides that cover the sequence of HocAST and identifies it unequivocally (Figure 3). The quaternary structure of the enzyme was analyzed by size-exclusion chromatography. The recombi-

Figure 3. Peptide mass fingerprint of HocAST. The sequence of the identified peptides is shaded and underlined. The molecular mass of each peptide is in [Da].

nant protein in the chromatographic column was eluted in two peaks at 100 and 150 mL (Figure S2). Peak 1 corresponds to the exclusion volume that contains oligomers of the protein. If the elution volume of peak 2 was interpolated into the calibration curve, a weight of approximately 40 kDa that corresponds to the monomer of HocAST was obtained (Figure S2).

The spectroscopic characterization of purified HocAST is shown in Figure 4. The far-UV circular dichroism (CD) spectrum shows two minima in ellipticity at approximately 210 and 220 nm, indicative of a main α/β secondary structure (Figure 4a).

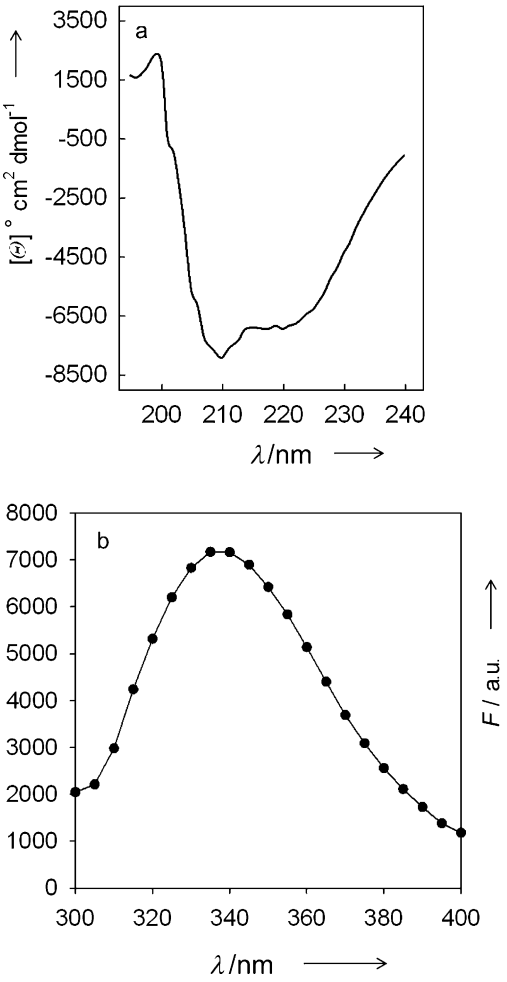

Figure 4. Spectroscopic characterization of recombinant HocAST. a) Far-UV CD spectrum. b) Tryptophan fluorescence emission spectrum; FI = fluorescence intensity.

The tertiary structure of the protein in the environment of the fluorophores was analyzed by fluorescence emission spectroscopy of the 12 tryptophan and 12 tyrosine residues contained in the sequence of HocAST (Figure 4b). Upon excitation at 275 nm, the spectrum exhibited an emission maximum centered at 335 nm, which is shifted approximately 15 nm from the position of the maximum described for free tryptophan in aqueous solution (348–350 nm).[15] This indicates that the average microenvironment of tryptophan in HocAST is significantly more hydrophobic than that of a residue completely exposed to the solvent. This blueshift of the fluorescence, together with the CD spectrum, supports the idea that the protein is expressed with proper folding. Moreover, emission spectra obtained upon excitation at 275 and 295 nm are practically identical, which indicates an almost negligible contribution of tyrosine residues to the fluorescence spectrum of the protein. This contribution, lower than expected for a Trp/Tyr ratio of 12:12, is probably because of an extensive resonance energy transfer from tyrosine fluorescence to nearby tryptophan residues and/or to quenching by other close side chains.

Biochemical characterization of HocAST

The course of the reaction catalyzed by the recombinant HocAST was followed in the sense of PAPS formation by monitoring the increase in absorbance at 405 nm caused by the appearance of *para*-nitrophenol(*p*-NP; **1**). The increase in absorbance was linear with enzyme concentration and reaction time. These results indicate clearly that HocAST was able to transfer the sulfuryl group from *p*-NPS to PAP (**2**) to show aryl sulfotransferase activity. The initial rate of the reaction measured over a range of substrate concentrations showed a Michaelis–Menten behavior (Figure S3). The apparent kinetics parameters of the HocAST enzyme were calculated independently for both substrates *p*-NPS and PAP (Table 1). It is difficult to compare these data with others reported in the literature as they are apparent parameters that are dependent on the conditions under which the assay was performed. Nevertheless, they are of the same order of magnitude as those reported for the sulfotransferase STF9 from *Mycobacterium avium*, another sulfotransferase that is also able to use PAPS and *p*-NPS as sulfuryl group donors.[16]

Table 1. Apparent kinetics parameters of HocAST for *p*-NPS and PAP.[a]

Substrate	K_M [μM]	V_{max} [μmol min^{-1} mg^{-1}]	$V_{max} K_M^{-1}$
p-NPS	45.9 ± 2.2	0.84 ± 0.008	0.018
PAP	4.0 ± 0.9	0.76 ± 0.015	0.19

[a] Kinetic parameters calculated at 25 °C and pH 7.0.

The recombinant HocAST exhibited activity between pH 6.0 and 7.5 with the maximum activity at pH 6.5. At pH values over 7.5, the activity drops drastically to virtually zero (Figure S4). To study the thermal stability of HocAST, the enzyme was incubated at 4, 25, 37, and 45 °C and their remnant activities were evaluated at room temperature (Figure 5). Therefore, we determined in this assay the progressive loss of activity caused by the irreversible denaturation of the enzyme.

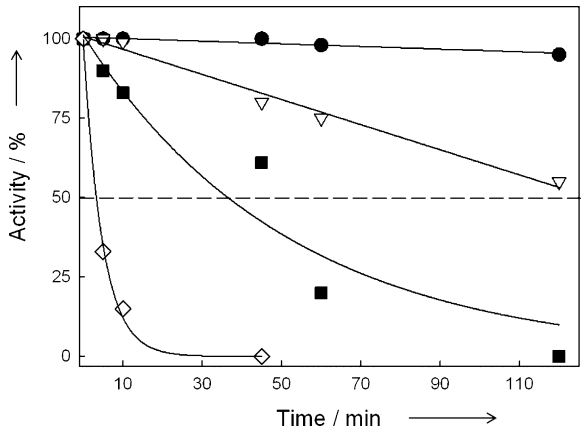

Figure 5. Thermal stability of the recombinant HocAST at 4 (●), 25 (▽), 37 (■), and 45 °C (◇).

The melting temperature of the recombinant HocAST was determined by thermal shift experiments at 33 °C (see Experimental Section and Figure S5). We observed a significant decrease of the half-life of the enzyme between 25 and 37 °C (Figure 5). At 25 °C the half-life of the sulfotransferase was over 3 h, but at 37 °C it was only 36–37 min, and at 45 °C less than 6 min (Figure 5). However, at 4 °C the enzyme retained over 90% of its activity for several days.

Substrate specificity studies

For this preliminary study of the HocAST substrate specificity, we assayed different commercially available phenolic compounds, aliphatic alcohols, and biologically relevant phosphorylated compounds that can be considered PAP analogs (Scheme 2).

Preliminary screening was performed by using a thermal shift assay.[17] The assay involves monitoring changes in the fluorescence signal of Sypro orange dye as it interacts with the hydrophobic core of a protein that is undergoing thermal unfolding. The melting temperature (T_m) of the protein will increase in the presence of ligands that bind to the properly folded protein. If an increase in T_m was detected, we performed the sulfation reaction as described in the Experimental Section, and the formation of the reaction product was confirmed by ESI-MS. The results are summarized in Table 2.

Table 2. Screening of HocAST acceptor specificity.

Compound	ΔT_m [°C]	Activity [%][a]
3	2.0	12.0
4	0.8	18.0
5	–[b]	n.a.[c]
6	–	n.a.
7	–	n.a.
10	–	n.a.
11	2.0	93.0
12	–	n.a.
13	–	n.a.
14	1.4	4.4
15	2.8	17.0
16	1.0	4.4
17	2.4	9.7
18	–	n.a.
19	–	n.a.

[a] 100% Activity is the maximum reaction rate with PAP as acceptor and *p*-NPS as sulfuryl donor. [b] –: No increase in T_m detected. [c] n.a.: Not applicable.

HocAST is able to transfer the sulfuryl group from *p*-NPS to the hydroxyl group of phenolic compounds with relatively good activity but aliphatic alcohols were not substrates of the enzyme. The best substrate was 4,4′-biphenol (**11**) probably because of the symmetry of the molecule. In the case of catechol (**4**), we could detect not only the monosulfated product, but also the disulfated one ([*M*+2$^+$] 191.2 and [*M*+1$^+$] 269.8, respectively). The assayed nucleoside triphosphates were good acceptors for the enzyme, and the results obtained indicate

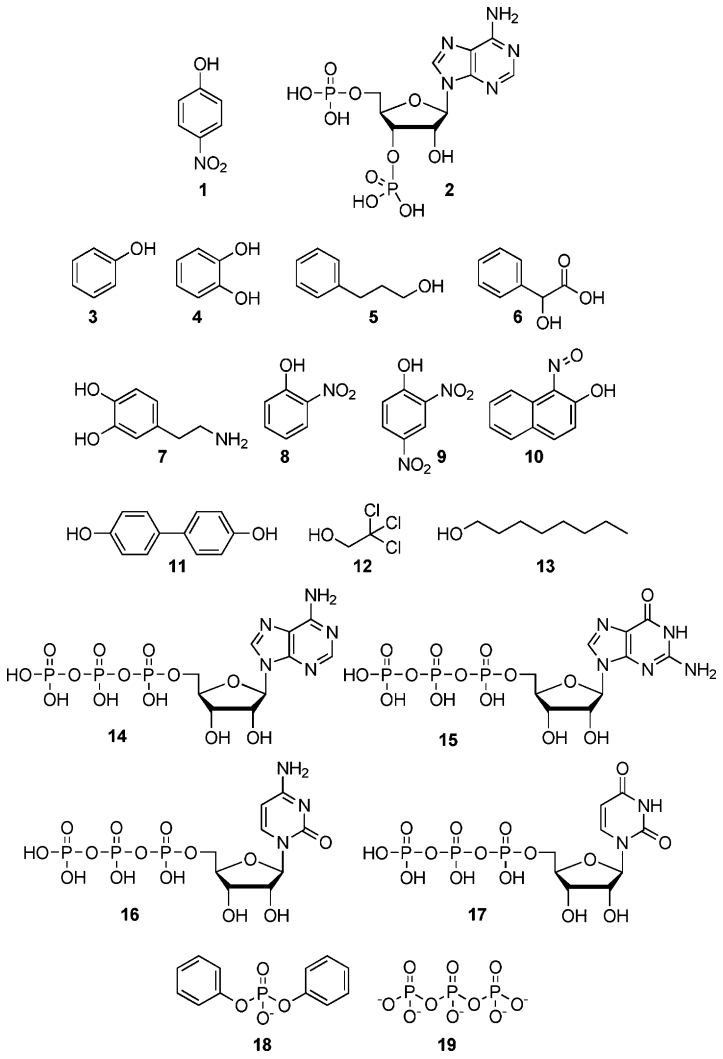

Scheme 2. Structure of the compounds assayed in this study as possible substrates of HocAST.

that the nucleoside moiety is needed to be recognized by the enzyme as triphosphate was neither ligand nor substrate.

Finally, we assayed the capacity of HocAST to transfer the sulfuryl group from PAPS to three different nitrophenols (**1**, **8**, and **9**). The activity with **1** was approximately half of that shown with *p*-NPS and PAP. With *o*-NP (**8**), the activity was quite similar but strongly decreased with dinitrophenol **9**, which showed a residual activity (≈2% of the activity shown with *p*-NPS).

Conclusions

We have shown experimentally that the gene Hoch_5094 from *Haliangium ochraceum* encodes for an aryl sulfotransferase. Circular dichroism analysis of the codified enzyme, HocAST, showed a main α/β secondary structure that agrees with the overall structure of other cytosolic sulfotransferases. HocAST is a very versatile enzyme as it is able to use both *p*-nitrophenyl sulfate and 3′-phosphoadenosine-5′-phosphosulfate as sulfuryl donors. With regard to the specificity towards the acceptor, HocAST has shown a broad scope and it is able to accept different phenolic compounds and nucleoside triphosphate as substrates. Therefore, HocAST is an interesting addition to the biocatalyst toolbox for the enzymatic sulfation of biologically relevant compounds.

Experimental Section

Materials and general procedures

E. coli BL21(DE3) competent cells were purchased from Stratagene Co. (US). Restriction enzymes, Taq polymerase and T4-DNA ligase were purchased from MBI Fermentas AB (Lithuania). PCR primers were purchased from Isogen Life Science (Spain), and the pET-28b(+) expression vector was purchased from Novagen. IPTG was purchased from Applichem GmBH (Germany). Plasmids and PCR purification kits were from Promega (US), and the DNA purification kit from agarose gels was from Eppendorf (Germany). SDS-PAGE was performed by using 10 and 5% acrylamide in the resolving and stacking gels, respectively. Gels were stained with Coomassie brilliant blue R-250 (Applichem GmBH, Germany). Electrophoresis was always run under reducing conditions in the presence of 5% β-mercaptoethanol. Nickel iminodiacetic acid (Ni^{2+}-IDA) agarose was supplied by Agarose Bead Technologies (Spain). All other compounds were purchased from Sigma–Aldrich and were used directly. Solvents were of analytical grade. DNA manipulation was performed according to standard procedures.[18]

Expression and purification of the aryl sulfotransferase from *Haliangium ochraceum*

Hoch_5094 gene was amplified by PCR by using an iCycler Thermal Cycler (MiniOpticon, BioRad) using genomic DNA from *Haliangium ochraceum* obtained from DSMZ (German Collection of Microorganisms and Cell cultures, DSM n° 14365) as a template. The forward primer (*Nde*I restriction site underlined) was

5′-TATAACATATGAATTCTACTGACGAACAACACA-3′

and the reverse primer (*Xho*I restriction site underlined) was

5′-CTCGAGTCAGTCCGGCAGCTCGCCG-3′.

PCR amplification was performed in 5 μL of reaction mixture that contained 20% DMSO and was subjected to 29 cycles of amplification. The cycle conditions were set as follows: denaturation at 94 °C for 1 min, annealing at 50 °C for 2 min, and elongation at 72 °C for 2 min. After digestion, the purified PCR product was ligated in the pET-28b(+) vector double-digested with the same restriction enzymes.

For the expression of the Hoch_5094 gene, transformed *E. coli* BL21 (DE3) cells, on the pET-AST6xHis plasmid, were grown in lysogeny broth (LB) medium supplemented with kanamycin (26 μg mL^{-1}) at 37 °C. When the culture reached an OD_{600} of 0.5–0.6, protein expression was induced with IPTG (0.4 mM), and the temperature was lowered to 30 °C. After 18 h, cells were harvested by centrifugation (3800×*g*) for 30 min at 4 °C. Cell pellets were resuspended in monosodium phosphate buffer (25 mM, pH 7.4) and treated with lysozyme and DNase for protein extraction.[19] The so-

lution was centrifuged for 40 min (8000×*g*, 4 °C) and collected for purification. The supernatant, which contained the recombinant protein, was loaded onto a Ni^{+2}-IDA-agarose column pre-equilibrated with sodium phosphate buffer (20 mM, pH 7.5). The recombinant ArylST was eluted with the same buffer that contained imidazole (500 mM). All the fractions that contained protein were pooled together and dialyzed to remove the imidazole. SDS-PAGE showed a single band that matched the expected molecular weight of the recombinant ArylST (37 kDa).

Sequence analysis and 3D modeling of HocAST

To analyze the sequence of HocAST, an alignment of four sequences was performed by using ClustalX.[20] The modeling of HocAST-was performed by using the SwissModel server with the best template option.

Protein analysis

Peptide mass fingerprint analysis from the SDS-PAGE band that corresponded to the hypothetical HocAST was performed at the Proteomic Unit of the Spanish National Center of Biotechnology (CNB-CSIC). Samples were digested with sequencing-grade trypsin O/N at 37 °C. Analysis by MALDI-TOF-MS produced peptide mass fingerprints, and the peptides observed can be collated and represented as a list of monoisotopic molecular weights. Data were collected in the *m/z* range of 800–3600.

The quaternary structure of HocAST was determined by size-exclusion chromatography under nondenaturing conditions. The protein was loaded into a HiLoad 26/60 SuperdexTM 75 PG column controlled by the AKTA-FPLC system (GE-Healthcare Life Science). The column was developed in phosphate buffer (50 mM, pH 7.2) that contained NaCl (0.15 M) at a constant flow rate of 1.0 mL min^{-1}. A calibration curve was plotted with the retention times of well-known proteins with molecular weights between 15 and 70 kDa.

CD and fluorescence spectroscopy

Far-UV CD spectra were recorded in the wavelength range of 195–250 nm by using a Jasco J-815 spectropolarimeter equipped with a constant-temperature cell holder Jasco PTC423-S Peltier. The protein concentration was 14 μM. The optical path length was 0.1 cm. The contribution of the buffer was always subtracted. For each sample, four spectra were accumulated at a scan speed of 20 nm min^{-1} with a bandwidth of 0.2 nm and averaged automatically. The mean residue ellipticity (Θ) is given in units of ° cm^2 $dmol^{-1}$. A value of 110 g mol^{-1} was used as the mean weight of the residue.

Tryptophan fluorescence emission spectra of HocAST were recorded by using a Jasco FP-8300 spectrofluorometer, and data were treated with the SpectraManager program. The contribution of the buffer was always subtracted. A quartz cell with a 1 cm path length in both the excitation (275 and 295 nm) and emission (295 to 400 nm) directions was used in all the experiments. The HocAST protein concentration was 10 μM in phosphate buffer (5.0 mM, pH 7.5), and experiments were performed at 25 °C.

Enzyme activity assays and steady-state kinetics analysis

The HocAST activity measurement was performed by using a high-throughput colorimetric 96-well plate assay. Sulfotransferase activity assays were performed at RT by following the increase of the absorbance at 405 nm ($\varepsilon_{p\text{-NP}} = 18\,000\ M^{-1}\,cm^{-1}$) for 15 min. In a total volume of 250 μL of reaction mixture, HEPES buffer (50 mM, pH 7.0), *p*-NPS (between 0 and 0.5 mM as indicated), and acceptor (between 0–0.02 mM as indicated) were added. The reactions were initiated by the addition of HocAST (50 μL, 14 μM). In all cases, the reaction was stopped by the addition of NaOH (50 μL, 1 N). For the determination of apparent kinetic constants (with the variation of only one substrate), initial velocities (V_0) were fitted to the Michaelis–Menten equation. Kinetics parameters were calculated by using the built-in nonlinear regression tools in SigmaPlot 11.0.

Substrate specificity studies

Thermal shift assays were performed by using an iQ5 Real Time Detection System (BioRad, CA). To monitor the protein unfolding, the fluorescent dye Sypro orange was used. The fluorescence signal of the dye is quenched in the aqueous environment of a properly folded protein in solution, but as the protein unfolds, it exposed its hydrophobic residues to the environment. The dye then binds to the hydrophobic regions and becomes unquenched. Acceptor solutions (5 μL, 10 mM) were added to Tris buffer (45 μL, 10 mM, pH 7.0) that contained Sypro Orange (0.5 μL in 0.5 mL) and protein (4.4 μM). The plates were heated from 25 to 70 °C at a rate of 0.2 °C min^{-1}. The fluorescence intensity was measured with excitation and emission wavelengths of 490 and 530 nm, respectively.

If a thermal shift was detected, sulfotransferase activity was confirmed by the colorimetric method described above. However, to determinate the activity of the HocAST using PAPS as the sulfuryl donor, the reaction mixtures contained phosphate buffer (184 μL, 50 mM, pH 7.0), PAPS (2.7 μL, 9 mM), and acceptor (7.5 μL, 1 mM). The reactions were initiated by the addition of HocAST (50 μL, 14 μM).

In all cases, the identity of the reaction products was confirmed by positive-ion ESI-MS spectrometry: *m/z*: PAPS 506.9 [M^+]; adenosine-5′-triphosfate 5′-sulfate (ATPS) 587 [M^+]; guanosine-5′-triphosphate-5′-sulfate (GTPS) 603 [M^+]; citidine-5′-triphosphate-5′-sulfate (CTPS) 563.9 [M^+]; uridina-5′-triphosphate-5′-sulfate (UTPS) 564.7 [M^+]; phenol sulfate 174.2 [M^+]; 4,4′-biphenol sulfate 266.0 [M^+]; catechol monosulfate 191.2 [M^{2+}]; catechol disulfate 269.8 [M^+]; *p*-nitrophenol sulfate 245.0 [NaM^+]; 2,4-dinitrophenol sulfate 280.6 [NaM^+]

Molecular docking studies

The crystal structure of the complex between human sulfotransferase SULT1A1 and PAP and of the mutant D249G with PAP and *p*-NP were obtained from the PDB (entries 3u3j and 3u3r, respectively). The receptor was prepared by using the Wizard tool of the Schrödinger suite. The initial conformations of PAP and *p*-NP were taken from the crystal structures. Subsequently, they were prepared by using LigPrep by modification of the torsions of the ligands and assignment of its appropriate protonation states. By using Glide, 32 stereochemical structures were generated per compound with possible states at target pH 7.0 ± 2.0 by using Ionizer, tautomerized, desalted, and optimized by the production of a low-energy 3D structure for the ligand under the OPLS 2005 force field[21] with retention of the specified chiralities of the input Maestro file. Then, a receptor grid was calculated for the prepared receptor such that various ligand poses bind within the predicted site during docking. By using Glide, grids were generated with the retention of the default parameters of a van der Waals scaling

factor of 1.00 and a charge cutoff 0.25 subjected to the OPLS 2001 force field. A cubic box of specific dimensions (15 Å×15 Å×15 Å) centered on the donor or acceptor was generated for the protein. After that, SP flexible ligand docking was performed by using Glide of Schrödinger-Maestro v9.2.7. Final scoring was performed on energy-minimized poses and displayed as a Glide score. The best-docked pose was recorded for the ligand.

Acknowledgements

We thank the Spanish Ministerio de Ciencia e Innovación (Grants PI11/01436 and CTQ2010-19073/BQU), Comunidad de Madrid (Grant S2009/PPQ-1752), and the MAPFRE Foundation for financial support. We thank Dr. Roland Wohlgemuth for the gift of PAPS and PAP. We thank the referees for their helpful comments.

Keywords: biocatalysis · bioorganic chemistry · biotransformations · enzymes · sulfation

[1] a) J. D. Mougous, R. E. Green, S. J. Williams, S. E. Brenner, C. R. Bertozzi, *Chem. Biol.* **2002**, *9*, 767 – 776; b) E. Chapman, M. D. Best, S. R. Hanson, C.-H. Wong, *Angew. Chem.* **2004**, *116*, 3610 – 3632; *Angew. Chem. Int. Ed.* **2004**, *43*, 3526 – 3548; c) V. L. Rath, D. Verdugo, S. Hemmerich, *Drug Discovery Today* **2004**, *9*, 1003 – 1011; d) M. W. Schelle, C. R. Bertozzi, *ChemBioChem* **2006**, *7*, 1516 – 1524; e) P. Bojarová, S. J. Williams, *Curr. Opin. Chem. Biol.* **2008**, *12*, 573 – 581.

[2] a) K. G. Bowman, C. R. Bertozzi, *Chem. Biol.* **1999**, *6*, R9 – R22; b) M. Negishi, L. G. Pedersen, E. Petrotchenko, S. Shevtsov, A. Gorokhov, Y. Kakuta, L. C. Pedersen, *Arch. Biochem. Biophys.* **2001**, *390*, 149 – 157; c) M. W. Duffel, A. D. Marshal, P. McPhie, V. Sharma, W. B. Jakoby, *Drug Metab. Rev.* **2001**, *33*, 369 – 395; d) W. W. Cleland, A. C. Hengge, *Chem. Rev.* **2006**, *106*, 3252 – 3278; e) J. G. McCarthy, E. B. Eisman, S. Kulkarni, L. Gerwick, W. H. Gerwick, P. Wipf, D. H. Sherman, J. L. Smith, *ACS Chem. Biol.* **2012**, *7*, 1994 – 2003.

[3] a) K. Kobashi, Y. Fukaya, D. H. Kim, T. Akao, S. Takebe, *Arch. Biochem. Biophys.* **1986**, *245*, 537 – 539; b) G. Malojčić, R. Glockshuber, *Antioxid. Redox Signaling* **2010**, *13*, 1247 – 1259; c) X. Tang, K. Eitel, L. Kaysser, A. Kulik, S. Grond, B. Gust, *Nat. Chem. Biol.* **2013**, *9*, 610 – 615.

[4] a) Y. Xu, S. Masuko, M. Takieddin, H. Xu, R. Liu, J. Jing, S. A. Mousa, R. J. Linhardt, J. Liu, *Science* **2011**, *334*, 498 – 501; b) P. L. DeAngelis, J. Liu, R. J. Linhardt, *Glycobiology* **2013**, *23*, 764 – 777.

[5] C.-H. Lin, G.-J. Shen, E. García-Junceda, C.-H. Wong, *J. Am. Chem. Soc.* **1995**, *117*, 8031 – 8032.

[6] a) M. A. van der Horst, J. F. T. van Lieshout, A. Bury, A. F. Hartog, R. Wever, *Adv. Synth. Catal.* **2012**, *354*, 3501 – 3508; b) P. Marhol, A. F. Hartog, M. A. van der Horst, R. Wever, K. Purchartová, K. Fuksová, M. Kuzma, J. Cvačka, V. Křen, *J. Mol. Catal. B* **2013**, *89*, 24 – 27; c) K. Purchartová, L. Engels, P. Marhol, M. Šulc, M. Kuzma, K. Slámová, L. Elling, V. Křen, *Appl. Microbiol. Biotechnol.* **2013**, DOI: 10.1007/s00253-013-4794-0.

[7] M. D. Burkart, M. Izumi, C.-H. Wong, *Angew. Chem.* **1999**, *111*, 2912 – 2915; *Angew. Chem. Int. Ed.* **1999**, *38*, 2747 – 2750.

[8] a) F. C. Kauffman, M. Whittaker, I. Anundi, R. G. Thurman, *Mol. Pharmacol.* **1991**, *39*, 414 – 420; b) E. Tan, S. K. Pang, *Drug Metab. Dispos.* **2001**, *29*, 335 – 346.

[9] N. Ivanova, C. Daum, E. Lang, B. Abt, M. Kopitz, E. Saunders, A. Lapidus, S. Lucas, T. Glavina Del Rio, M. Nolan, H. Tice, A. Copeland, J. F. Cheng, F. Chen, D. Bruce, L. Goodwin, S. Pitluck, K. Mavromatis, A. Pati, N. Mikhailova, A. Chen, K. Palaniappan, M. Land, L. Hauser, Y. J. Chang, C. D. Jeffries, J. C. Detter, T. Brettin, M. Rohde, M. Göker, J. Bristow, V. Markowitz, J. A. Eisen, P. Hugenholtz, N. C. Kyrpides, H. P. Klenk, *Stand. Genomic Sci.* **2010**, *2*, 96 – 106.

[10] Y. Kakuta, L. G. Pedersen, C. W. Carter, M. Negishi, L. C. Pedersen, *Nat. Struct. Biol.* **1997**, *4*, 904 – 908.

[11] N. Hempel, N. Gamage, J. L. Martin, M. E. McManus, *Int. J. Biochem. Cell Biol.* **2007**, *39*, 685 – 689.

[12] a) M. C. Peitsch, *Biotechnology* **1995**, *13*, 658 – 660; b) K. Arnold, L. Bordoli, J. Kopp, T. Schwede, *Bioinformatics* **2006**, *22*, 195 – 201; c) F. Kiefer, K. Arnold, M. Künzli, L. Bordoli, T. Schwede, *Nucleic Acids Res.* **2009**, *37*, D387 – D392.

[13] T. Teramoto, Y. Sakakibara, M.-C. Liu, M. Suiko, M. Kimura, Y. Kakuta, *Biochem. Biophys. Res. Commun.* **2009**, *383*, 83 – 87.

[14] a) R. A. Friesner, J. L. Banks, R. B. Murphy, T. A. Halgren, J. J. Klicic, D. T. Mainz, M. P. Repasky, E. H. Knoll, M. Shelley, J. K. Perry, D. E. Shaw, P. Francis, P. S. Shenkin, *J. Med. Chem.* **2004**, *47*, 1739 – 1749; b) T. A. Halgren, R. B. Murphy, R. A. Friesner, H. S. Beard, L. L. Frye, W. T. Pollard, J. L. Banks, *J. Med. Chem.* **2004**, *47*, 1750 – 1759; c) R. A. Friesner, R. B. Murphy, M. P. Repasky, L. L. Frye, J. R. Greenwood, T. A. Halgren, P. C. Sanschagrin, D. T. Mainz, *J. Med. Chem.* **2006**, *49*, 6177 – 6196.

[15] J. R. Lakowicz, *Principles of Fluorescence Spectroscopy*, Plenum Press, New York, **1999**.

[16] Md. M. Hossain, Y. Moriizumi, S. Tanaka, M. Kimura, Y. Kakuta, *Mol. Cell. Biochem.* **2011**, *350*, 155 – 162.

[17] a) F. H. Niesen, H. Berglund, M. Vedadi, *Nat. Protoc.* **2007**, *2*, 2212 – 2221; b) J. K. Kranz, C. Schalk-Hihi, *Methods Enzymol.* **2011**, *493*, 277 – 298.

[18] J. Sambrook, E. F. Fritsch, T. Maniatis, *Molecular Cloning. A Laboratory Manual, 2nd ed.*, Cold Spring Harbor Laboratory Press, Cold Spring Harbor, **1989**.

[19] A. Bastida, A. Fernández-Mayoralas, R. Gómez, F. Iradier, J. C. Carretero, E. García-Junceda, *Chem. Eur. J.* **2001**, *7*, 2390 – 2397.

[20] M. A. Larkin, G. Blackshields, N. P. Brown, R. Chenna, P. A. McGettigan, H. McWilliam, F. Valentin, I. M. Wallace, A. Wilm, R. Lopez, J. D. Thompson, T. J. Gibson, D. G. Higgins, *Bioinformatics* **2007**, *23*, 2947 – 2948.

[21] a) W. L. Jorgensen, J. Tirado-Rives, *J. Am. Chem. Soc.* **1988**, *110*, 1657 – 1666; b) W. L. Jorgensen, D. S. Maxwell, J. Tirado-Rives, *J. Am. Chem. Soc.* **1996**, *118*, 11225 – 11236; c) D. Shivakumar, J. Williams, Y. Wu, W. Damm, J. Shelley, W. Sherman, *J. Chem. Theory Comput.* **2010**, *6*, 1509 – 1519.

Received: October 8, 2013
Revised: December 13, 2013
Published online on March 26, 2014